Am J Transl Res 2015;7(4):697-709
www.ajtr.org /ISSN:1943-8141/AJTR0004983

*Original Article*

# VEGF-C/VEGFR-3 pathway promotes myocyte hypertrophy and survival in the infarcted myocardium

Tieqiang Zhao[1], Wenyuan Zhao[1], Weixin Meng[1], Chang Liu[1], Yuanjian Chen[1], Ivan C Gerling[2], Karl T Weber[1], Syamal K Bhattacharya[1], Rahul Kumar[1], Yao Sun[1]

*Divisions of [1]Cardiovascular Diseases, [2]Endocrinology, Department of Medicine, University of Tennessee Health Science Center, Memphis, TN 38163, USA*

Received December 17, 2014; Accepted April 11, 2015; Epub April 15, 2015; Published April 30, 2015

**Abstract:** Background: Numerous studies have shown that in addition to angio/lymphangiogenesis, the VEGF family is involved in other cellular actions. We have recently reported that enhanced VEGF-C and VEGFR-3 in the infarcted rat myocardium, suggesting the paracrine/autocrine function of VEGF-C on cardiac remodeling. The current study was designed to test the hypothesis that VEGF-C regulates cardiomyocyte growth and survival in the infarcted myocardium. Methods and results: Gene profiling and VEGFR-3 expression of cardiomyocytes were assessed by laser capture microdissection/microarray and immunohistochemistry in the normal and infarcted myocardium. The effect of VEGF-C on myocyte hypertrophy and apoptosis during normoxia and hypoxia was detected by RT-PCR and western blotting in cultured rat neonatal cardiomyocytes. VEGFR-3 was minimally expressed in cardiomyocytes of the normal and noninfarcted myocardium, while markedly elevated in the surviving cardiomyocytes of the infarcted myocardium and border zone. Genes altered in the surviving cardiomyocytes were associated with the networks regulating cellular growth and survival. VEGF-C significantly increased the expression of atrial natriuretic factor (ANP), brain natriuretic factor (BNP), and β-myosin heavy chain (MHC), markers of hypertrophy, in neonatal cardiomyocytes. Hypoxia caused neonatal cardiomyocyte atrophy, which was prevented by VEGF-C treatment. Hypoxia significantly enhanced apoptotic mediators, including cleaved caspase 3, 8, and 9, and Bax in neonatal cardiomyocytes, which were abolished by VEGF-C treatment. Conclusion: Our findings indicate that VEGF-C/VEGFR-3 pathway exerts a beneficial role in the infarcted myocardium by promoting compensatory cardiomyocyte hypertrophy and survival.

**Keywords:** VEGF-C, cardiomyocytes, myocardial infarction, hypertrophy, apoptosis

## Introduction

Ventricular dysfunction appears most commonly in patients who have had a previous myocardial infarction (MI). Multiple factors contribute to the development of cardiac failure following MI, including infarct size, structural remodeling, and impaired cardiac repair [1]. In addition to necrotic cardiomyocytes induced by hypoxia, the region between the infarcted and noninfarcted myocardium is also under stress. These cardiomyocytes are under hypoxic conditions and surrounded by inflammatory and fibroblast-like cells, which release large amounts of cytokines, growth factors, and reactive oxygen species (ROS) [2, 3]. These substances may exert protective or detrimental effects on the surviving cardiomyocytes in the infarcted myocardium and border zone. For example, ROS can further damage cardiomyocytes, extending into the infarct zone [4]. The potential protective role of local factors on cardiomyocytes, however, remains unknown.

The VEGF is a sub-family of growth factors composed of five different isoforms: VEGF-A, -B, -C, -D and placenta growth factor. VEGF initiates cellular responses by interacting with tyrosine kinase receptors on the cell surface. There are three main VEGF receptor subtypes, VEGFR-1, -2, and -3. VEGF-A binds to VEGFR-1 and -2; VEGF-B is the ligand of VEGFR-1; while VEGF-C and -D bind to VEGFR-2 and -3. VEGF-A and -B are the key mediators of angiogenesis, while VEGF-C and -D are recognized to stimulate lymphangiogenesis in physiological and pathological conditions [5, 6].

Numerous studies have shown that in addition to angio/lymphangiogenesis, the VEGF family is

involved in other cellular actions [7-9]. A recent study by our group showed that VEGF-C and VEGFR-3 levels are significantly increased in the infarcted myocardium [10]. In addition to lymphatic vessels, VEGFR-3 is highly expressed in cardiomyocytes and myofibroblasts, indicating that VEGF-C plays an autocrine/paracrine role in the regulation of myocyte and myofibroblast function and growth/survival. These observations demonstrate that besides lymphangiogenesis, VEGF-C is also involved in other cellular actions in the infarcted heart. Another recent study of ours further revealed that VEGF-C stimulates cardiac fibrogenesis by inducing myofibroblast proliferation and collagen synthesis, thus promoting cardiac repair [10]. The potential regulation of VEGF-C on cardiomyocytes in the infarcted heart, however, remains unknown. Using an experimental infarcted rat heart model and cultured neonatal rat cardiomyocytes, the current study was designed to test the hypothesis that VEGF-C promotes myocyte hypertrophy and survival during hypoxia.

## Materials and methods

### *Animal model*

The study was approved by the University of Tennessee Health Science Center Animal Care and Use Committee. A left ventricular anterior transmural MI was created in 8-week-old male Sprague-Dawley rats (Harlan, Indianapolis, IN) *via* permanent ligation of the left coronary artery. Animals were anesthetized with 1.5% isoflurane, intubated and ventilated with a rodent respirator. The heart was exposed *via* a left thoracotomy and the left anterior descending coronary artery was ligated with a 6-0 silk suture. The chest was then closed and the lungs were re-inflated using positive end-expiratory pressure [11]. This surgical procedure leads to free wall infarction (40-45% of left ventricle). Sham-operated rats served as controls. Rats with an MI were sacrificed at postoperative week 2 (n = 6/group). Hearts were removed and snap-frozen at -80°C until further use.

### *Histology and immunofluorescence*

Cryostat coronal sections (6 μm) of the normal and infarcted hearts were prepared and cardiac morphology was examined using hematoxylin and eosin staining. Myocyte diameter in the normal and infarcted myocardium was determined using image processing software (NIH image 1.60) [12].

Cells expressing VEGFR-3 in the normal and infarcted hearts were determined by fluorescent immunohistochemistry. Cryostat coronal sections (6 μm) were prepared and blocked in 1% bovine serum albumin. Rabbit anti-VEGFR-3 antibody (Santa Cruz, Santa Cruz, CA) was applied and revealed by Cy3-labeled anti-rabbit IgG (Sigma, St. Louis, MO). Samples were examined using a laser-scanning confocal imaging system (Zeiss LSM510) [10].

### *Laser capture microdissection and RNA extraction*

Cryostat coronal sections of hearts (10 μm) were prepared and dehydrated. Cardiomyocytes were captured from the normal and infarcted myocardium with the ArcturusXT™ Microdissection System. The infrared laser captured cells onto CapSure LCM caps. Cells collected from four sections at each site were pooled for Affymetrix microarray analyses. RNA trapped in the CapSure LCM caps was extracted using the PicoPure RNA isolation kit; RNA quality was analyzed using Bioanalyzer (Model 2100, Agilent, Foster City, CA) [13].

### *Microarray analysis*

Total RNA was processed using standard protocols and hybridized to the Affymetrix Rat Genome 230 2.0 Array. This array is comprised of more than 31,000 probe sets, analyzing over 30,000 transcripts and variants from over 28,000 well-substantiated rat genes. Probe set level intensity values were extracted from the CEL files using the Affymetrix Gene Chip Operating Software. Fold change of MI vs normal myocardium was calculated [14].

### *Analyses of molecular networks*

Ingenuity pathway analysis (IPA) was used to identify the functions of those genes differentially expressed in surviving cardiomyocytes of the infarcted myocardium compared to those in the normal myocardium. Selected genes with unique gene identifiers (Agilent probe set ID) and their corresponding fold-change values were uploaded as a tab-delimited text file where the gene identifiers were mapped to

their corresponding gene object in the Ingenuity database. These were then called "focus genes" and used as starting points in order to query the database to generate biological networks with a statistical score provided for each network [14, 15].

*qPCR*

Total RNA was extracted from the normal and infarcted myocardium using Trizol Reagent (Invitrogen, Carlsbad, CA). RNA was treated with DNase using a TURBO DNA-free kit (Ambion, Austin, TX), and purified with an RNeasy Mini Kit (Qiagen Inc, Valencia, CA). Purification, concentration and integrity of the RNA were examined with a NanoDrop spectrophotometer (Thermo Scientific, Wilmington, DE), and Agilent Bioanalyzer (Agilent Technologies, Foster City, CA), respectively. cDNA was prepared from total RNA using a High Capacity cDNA reverse transcriptase kit (Applied Biosystems, Foster City, CA). The gene-specific probes and primer sets for skeletal actin, ANP and BNP were deduced using Universal ProbeLibrary Assay Design software (https://www.roche-applied-science.com). ANP and BNP mRNA levels were detected and analyzed on an LightCycler 480 System (Roche, Indianapolis, IN) under the following cycling conditions: 1 cycle at 95°C for 5 min and then 45 cycles at 95°C for 10 s, 60°C for 30 s, and 72°C for 10 s. The PCR mix contained 0.2 μl of 10 μM primers, 0.1 μl of 10 μM Universal library probe, 5 μl of LC 480 master mix (2X), 2 μl of template cDNA, and RNase-free water to 10 μl. TATA box-binding protein was selected as the endogenous quantity control. Fold change was used to compare the difference between the two groups [16].

*Primary culture of rat ventricular cardiomyocytes*

Primary cultures of left ventricular cardiomyocytes were prepared from one day old Sprague-Dawley rat pups. The rat pups were euthanized and hearts were removed and minced into small pieces. Cells were isolated by serial digestion in collagenase II (25 mg/100 ml) and trypsin (40 mg/100 ml) at 37°C with shaking at 75 rpm. After 6-8 digestions, the cell suspensions are pooled and centrifuges at 200 g for 5 min. The pellet was re-suspended in plating media (Dulbecco's modified Eagle's medium (DMEM)/F-12 supplemented with 10% fetal bovine serum). The suspension was passed through a 70 um nylon filter and pre-plated for 75 min. The myocyte-enriched fraction were then collected and seeded onto gelatin pre-coated plates. The density was 750 K per well in a six-well plate. Cell purity was detected by immunohistochemical α-myosin heavy chain, vimentin, α-smooth muscle actin and CD31 staining. Over 95% of cells were identified to be cardiomyocytes. Cultures were maintained at 37°C in 95% humidified air and 5% $CO_2$ atmosphere [17, 18].

*Hypoxia and treatment*

The cells were starved for 20 hr with serum free media before treatment. VEGF-C (200 ng/ml) was administered to the serum-free media with or without hypoxia. For hypoxia, the media was changed to serum-free DMEM/F12 saturated with 95% $N_2$/5% $CO_2$, and cells were placed in a hypoxia chamber (Billups-Rothenberg) saturated with 95% $N_2$/5% $CO_2$ at 37°C for 20 hr [19].

*Western blot*

Cells were washed twice with ice-cold PBS and scraped into modified RIPA buffer. Protein extracts were recovered following centrifugation. Aliquots of proteins (10-20 μg) were separated on 12% sodium dodecyl sulfate polyacrylamide gels (SDS/PAGE) and transferred to polyvinylidene difluoride (PVDF) membranes. Membranes were blocked for nonspecific protein with 5% nonfat dry milk in TBS and then probed overnight at 4°C with primary antibodies against cleaved caspase 3, 8, 9 (Cell Signaling, Danvers, MA), Bax (R&D, Minneapolis, MN), ANP, β-MHC (Millipore, Bellerica, MA) and α-actin (Sigma, St. Louis, MO). Membranes were then washed in triplicate (10 min/wash) with TBS with 0.05% Tween 20 to remove unbound antibodies and then further incubated with appropriate HRP-conjugated secondary antibody (1:2,000). Membranes were developed using a chemoluminescence reagent kit (Amersham Pharmacia Biotech, Piscataway, NJ) according to the manufacturer's protocol. The amount of protein detected was assessed by quantitative densitometry and analyzed by NIH Image J software, which gives integrated optical density [16].

*Cultured cardiomyocyte size determination*

Cardiomyocytes were seeded onto the gelatin-coated glass coverslips, allowed to grow for

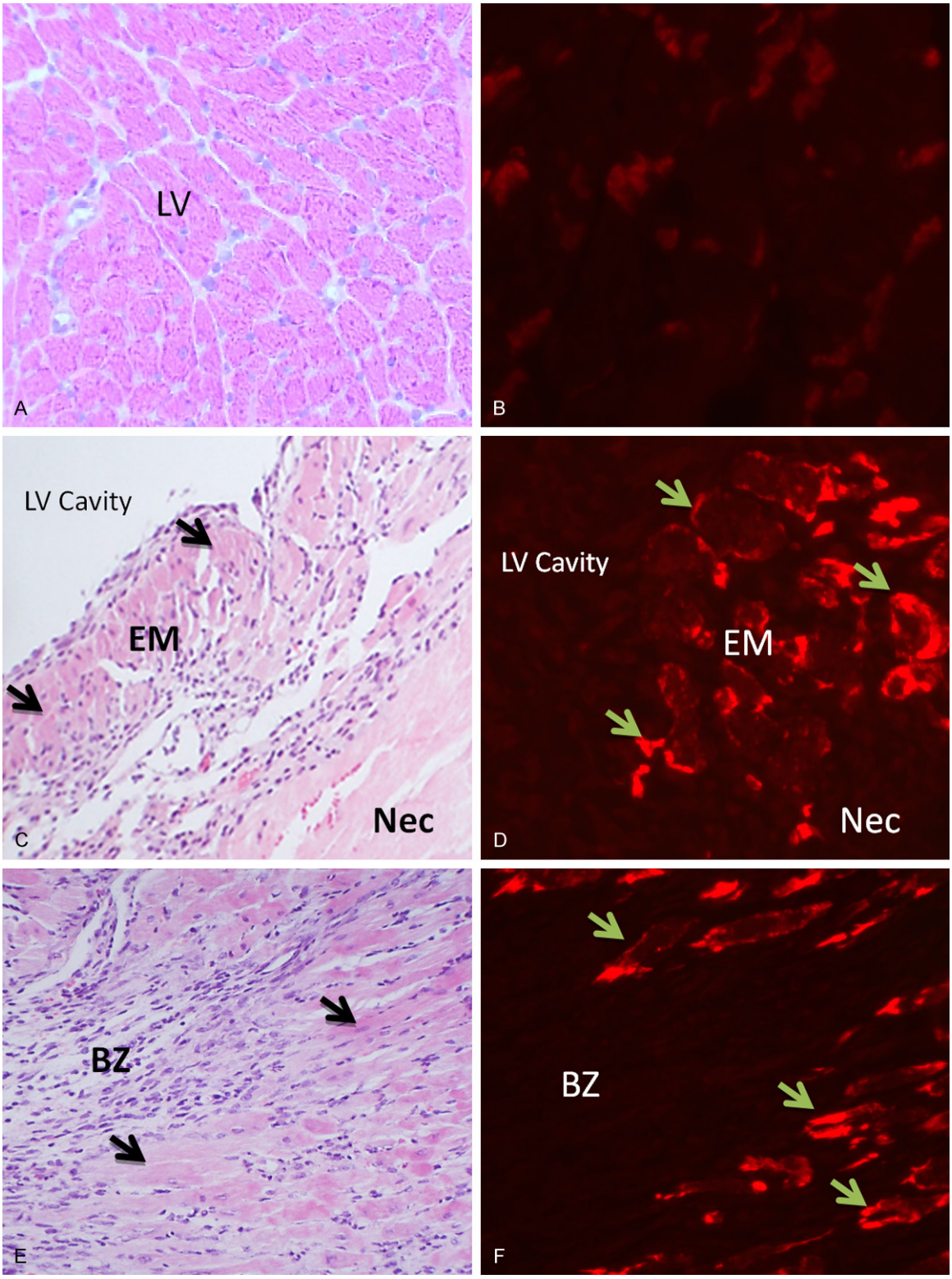


**Figure 1.** Cardiac morphology and VEGFR-3 expression. Following MI, a number of cardiomyocytes survived in the endocardium (EM) of the infarcted myocardium (panel C, arrows) and border zone (BZ) (panel E, arrows). Compared to the normal myocardium with low levels of VEGFR-3 (panel B), the surviving cardiomyocytes of the infarcted myocardium (panel D) and border zone (panel F) expressed high levels of VEGFR-3. (Panel A) normal myocardium; LV: left ventricle; Nec: necrotic myocardium. Magnifications: 200 ×.

**Table 1.** Altered network pathways in the surviving cardiomyocytes of the infarcted myocardium

| Network | Molecular in network | SScore | Focus molecule | Top diseases and functions |
|---|---|---|---|---|
| 1 | CAP1, CGNL1↑, DESI1, DLX2, Eef1a1, GORASP1, IDH2, IRF2BP1, KCNA6↑, KCNAB2, LEPREL1↑, LEPREL2↑, LEPREL4↑, LRRC16A↑, MFAP3L↑, MXRA8↑, MYEF2, NARS, NOP58, PNP, POLD3, RGD1561333↑, SEMA5A↑, SLC41A2↑, SMCHD1, TEAD1, TMED3↑, TMEM2↑, TMEM45A↑, TP53BP2, UBC, USP25, VWA5A↑, ZMIZ1 | 222 | 15 | Hereditary disorder, ophthalmic disease, cardiovascular system development and function |
| 2 | ADARB1↑, APOE↑, ARID5B↑, E2f, FRZB↑, growth hormone, Hdac, HDL, HDL-cholesterol, histone h4, Jnk, LDL, LDLR↑, N-cor, NOX4↑, PFKP↑, PLVAP↑, pro-inflammatory cytokine, ROBO2↑, Scd2↑, SFRP, SFRP1↑, SFRP2↑, SLC16A3↑, T3-TR-RXR, TNNI1↑, wnt | 220 | 14 | Dermatological diseases and conditions, metabolic disease, cellular growth and proliferation |
| 3 | Calpain, CAPN6↑, CTHRC1↑, CX3CR1↑, EFNA5↑, estrogen receptor, fibrinogen, FN1↑, focal adhesion kinase, FZD2↑, Gpcr↑, GPR176↑, GPRC5A↑, P38 MAPK, PAK1↑, Rac, Ras homolog, RGS1↑, RPL3↑, RPLP0↑, RPS27↑, SERPINE2↑, SLIT3↑, TCR, trypsin | 119 | 15 | Cell morphology, cellular assembly and organization, cellular development |
| 4 | CDH1, CKMT2, COL6A3↑, EPO, ERBB2, Fcrls↑, Hamp↑, IL6, IL10, IL20, IL17RA, INSR, JAK, JAK2, KCNV2↑, LOXL3↑, LRIG3, mir-373↑, OLFML3↑, PTGER3↑, REG3A↑, SLAMF9↑, ST8SIA2↑, UNC5B↑ | 116 | 12 | Gene expression, cellular movement, hematological system development and function |
| 5 | CLEC11A↑, Fcer1, FLT4↑, Gm-csf, Gp49a/Lilrb4↑, growth factor receptor, H19↑, Iga, Ige, Integrin, MDK↑, MTHFD2↑, MYO1D↑, dgfr, PDGFRB↑, PI3K (complex), Ras, Reg3g↑, Shc, SHC1↑, Sos, TSPAN4↑ | 115 | 11 | Cardiovascular system development and function, organismal development, tissue morphology |
| 6 | Caspase, Cpla2, GOT, Hbq1↑, hemoglobin, IL1, IL12 (complex), interferon alpha, KIRREL↑, LGALS3BP↑, mir-21↑, NAIP↑, PTGS2↑, SRC (family), STAT5a/b, UNC5B↑, Vegf | 111 | 9 | Cell morphology, cell death and survival, cellular movement |

↑: Increased gene expression.

**Table 2.** Increased expression of genes in the surviving cardiomyocytes of the infarcted myocardium

| Symbol | Gene name | Symbol | Gene name |
|---|---|---|---|
| ADARB1 | Adenosine ddeaminase, RNA-specific, B1 | mir-21 | Microrna 21 |
| APOE | Apolipoprotein E | mir-373 | Microrna 373 |
| ARID5B | AT rich Interactive domain 5B (MRF1-Like) | MTHFD2 | Methylenetetrahydrofolate dehydrogenase 2 |
| CAP1 | Adenylate cyclase-associated protein 1 (Yeast) | MXRA8 | Matrix-remodelling associated 8 |
| CAPN6 | Calpain 6 | MYEF2 | Myelin expression factor 2 |
| CDH1 | Cadherin 1, type 1, E-cadherin (Epithelial) | MYO1D | Myosin ID |
| CGNL1 | Cingulin-Like 1 | NAIP | NLR family, apoptosis inhibitory protein |
| CKMT2 | Creatine kinase, mitochondrial 2 (Sarcomeric) | NARS | Asparaginyl-Trna synthetase |
| CLEC11A | C-type lectin domain family 11, member A | N-COR | Nuclear receptor corepressor |
| COL6A3 | Collagen, type vi, alpha 3 | NOP58 | NOP58 ribonucleoprotein |
| CPLA2 | Cytosolic phospholipase A2 | NOX4 | NADPH oxidase 4 |
| CTHRC1 | Collagen triple helix repeat containing 1 | OLFML3 | Olfactomedin-Like 3 |
| CX3CR1 | Chemokine (C-X3-C motif) receptor 1 | P38 MAPK | P38 mapkinase |
| DESI1 | Desumoylating isopeptidase 1 | PAK1 | P21 protein (Cdc42/Rac)-activated kinase 1 |
| DLX2 | Distal-less homeobox 2 | PDGFR | Platelet-derived growth factor receptor |
| DOCK8 | Dedicator of cytokinesis 8 | PDGFRB | Platelet-derived frowth factor receptor, beta |
| E2F | E2F Transcription Factor | PFKP | Phosphofructokinase, platelet |
| EEF1A1 | Eukaryotic translation elongation factor 1 alpha 1 | PI3K | Phosphoinositide 3-kinase complxe |
| EFNA5 | Ephrin-A5 | PLVAP | Plasmalemma vesicle associated Protein |
| EPO | Erythropoietin | PNP | Purine nucleoside phosphorylase |
| ERBB2 | V-Erb-B2 avian erythroblastic leukemia viral oncogene 2 | POLD3 | Polymerase (DNA-directed), delta 3 |
| FAT1 | FAT atypical cadherin 1 | PTGER3 | Prostaglandin E receptor 3 (Subtype EP3) |
| FCER1 | Fc fragment of ige, high affinity I | PTGS2 | Prostaglandin-endoperoxide synthase 2 |
| FCRLS | Fc receptor-like s, scavenger receptor | RAC | Ras-related protein |
| FLT4 | Fms-related tyrosine kinase 4 | RAS | Small gtpase from rat sarcoma |
| FN1 | Fibronectin 1 | RAS | Small gtpase from rat sarcoma homolog |
| FRZB | Frizzled-related protein | REG3A | Regenerating islet-derived 3 alpha |
| FZD2 | Frizzled family receptor 2 | REG3G | Regenerating islet-derived 3 Gamma |
| GM-CSF | Granulocyte-macrophage Colony-Stimulating-Factor | RGD1561333 | Similar to 60S ribosomal protein L8 |
| GORASP1 | Golgi reassembly stacking protein 1, 65 kda | RGS1 | Regulator of G-protein signaling 1 |
| GP49A/LIL | Leukocyte immunoglobulin-like receptor, subfamily B | ROBO2 | Roundabout, axon guidance Receptor, Homolog 2 |
| GPCR | G-Protein coupled receptor | RPL3 | Ribosomal protein L3 |
| GPR176 | G Protein-coupled receptor 176 | RPLP0 | Ribosomal protein, large, P0 |
| GPRC5A | G Protein-coupled receptor, family C, group 5A | RPS27 | Ribosomal protein S27 |
| H19 | Imprinted maternally expressed transcript | SCD2 | Stearoyl-coenzyme a desaturase 2 |
| HAMP | Hepcidin antimicrobial peptide | SEMA5A | Semaphorin 5A |
| HBQ1 | Hemoglobin, theta 1 | SERPINE2 | Serpin peptidase inhibitor, clade E 2 |
| HDAC1 | Histone deacetylase | SFRP | Secreted frizzled-related protein |
| HDL | High density lipoprotein | SFRP1 | Secreted frizzled-related protein 1 |
| IDH2 | Isocitrate dehydrogenase 2 | SFRP2 | Secreted frizzled-related protein 2 |
| IGA | Immunoglobulin A | SHC | Squalene-hopene cyclase |
| IGE | Immunoglobulin E | SHC1 | SHC (Src homology 2 domain containing) 1 |
| IL1 | Interleukin 1 | SLAMF9 | SLAM Family Member 9 |
| IL10 | Interleukin 10 | SLC16A3 | Solute carrier family 16, member 3 |
| IL12 | Interleukin 12 | SLC41A2 | Solute carrier family 41, member 2 |
| IL17RA | Interleukin 17 receptor A | SLIT3 | Slit homolog 3 (drosophila) |
| IL20 | Interleukin 20 | SMCHD1 | Structural maintenance of chromosomes 1 |
| IL6 | Interleukin 6 (Interferon, Beta 2) | SOS | Son of sevenless |
| INSR | Insulin receptor | SRC | V-Src sarcoma viral oncogene |
| IRF2BP1 | Interferon regulatory factor 2 binding Protein 1 | ST8SIA2 | ST8 sialyltransferase 2 |
| JAK | Janus kinase | STAT5A/B | Signal transducer, activator of transcription5A/B |
| JAK2 | Janus kinase 2 | T3-TR-RXR | T3-throid hormone receptor-retinoid X receptor |
| JNK | C-Jun N-terminal kinase | TEAD1 | TEA domain family member 1 |
| K | Potassium voltage-gated channel | TM | Transmembrane Emp24 protein |
| KCNAB2 | Potassium voltage-gated channel, beta member 2 | TMEM2 | Transmembrane protein 2 |

| | | | |
|---|---|---|---|
| KCNV2 | Potassium channel, subfamily v, member 2 | TMEM45A | Transmembrane protein 45A |
| KIRREL | Kin of IRRE like (Drosophila) | TNNI1 | Troponin I Type 1 (Skeletal, Slow) |
| LDL | Low density lipoprotein | TP53BP2 | Tumor Protein P53 Binding Protein, 2 |
| LDLR | Low density lipoprotein receptor | TSPAN4 | Tetraspanin 4 |
| LEPREL1 | Leprecan-like 1 | UBC | Ubiquitin C |
| LEPREL2 | Leprecan-like 2 | UNC5B | Unc-5 homolog B (C. Elegans) |
| LEPREL4 | Leprecan-like 4 | UNC5B | Unc-5 homolog B (C. Elegans) |
| LGALS3BP | Lectin, galactoside-binding, soluble, 3 Binding Protein | USP25 | Ubiquitin specific peptidase 25 |
| LOXL3 | Lysyl oxidase-like 3 | VEGF | Vascular endothelial growth factor |
| LRIG3 | Leucine-rich repeatsm, immunoglobulin-like domains 3 | VWA5A | Von willebrand factor a domain containing 5A |
| LRRC16A | Leucine rich repeat containing 16A | WNT | Wingless-related integration site |
| MDK | Midkine (Neurite growth-promoting factor 2) | ZMIZ1 | Zinc finger, MIZ-type containing 1 |

24-48 hr, and acquiesced. Following treatment with hypoxia and/or VEGF-C, cells were fixed with 10% formalin for 10 min, washed in PBS containing 1% Triton X-100 for 10 min, and blocked with 2% BSA in PBS. After washing with PBS, cells were incubated with primary antibody mouse anti-α-actinin (Sigma, St. Louis, MO). FITC conjugated goat anti-mouse secondary antibody was used. Fluorescence images of cells were captured using a laser-scanning confocal image system (Zeiss LSM510). Cell size was measured using the NIH Image J software. Approximately 100 cells were measured in each group [20].

*Statistical analyses*

Statistical analyses of PCR, western blot, and cardiomyocyte size data among groups was performed using analysis of variance. Values are expressed as mean ± SEM with $p < 0.05$ considered statistically significant. Multiple group comparisons among controls and each group were made using the Scheffé's *F*-test.

## Results

*Cardiac morphology*

Left coronary artery ligation leads to transmural infarction of the left ventricle. However, a certain amount of cardiomyocytes in the endocardium of the infarcted myocardium (**Figure 1C**) and the border zone (**Figure 1E**) remained viable. These cells were co-localized with the repairing cells including inflammatory, fibroblast-like and endothelial cells.

*Spatial expression of VEGFR-3 in cardiomyocytes following MI*

A previous study by our group showed that VEGFR-3 density was significantly increased in the infarcted myocardium as detected using *in vitro* quantitative autoradiography [10]. Our current study further determined VEGFR-3 expression in cardiomyocytes of the normal, noninfarcted and infarcted myocardium by immunohistochemistry. We found that cardiomyocytes in the normal (**Figure 1B**) and noninfarcted myocardia (not shown) barely expressed VEGFR-3. However, surviving cardiomyocytes of the infarcted myocardium (**Figure 1D**) and border zone (**Figure 1F**) expressed high levels of VEGFR-C.

*Myocyte gene expression profiling*

Myocyte gene expression profiles were obtained by laser capture micro-dissection of cells followed by microarray analysis. We compared the gene expression profiles of cardiomyocytes between the infarcted and normal heart. Using a 1.5 fold change threshold, 82 genes were differentially expressed in the surviving cardiomyocytes of the infarcted myocardium. Of those, 75 out of 82 genes were up-regulated. Ingenuity analyses of the up-regulated genes produced six pathway networks associated with increased expression of genes in cardiomyocytes of the infarcted myocardium. Each network, summarized in **Table 1**, includes all genes in that network, genes altered in cardiomyocytes of the infarcted myocardium, statistical score, and top functions of the network. Gene symbols and names for each gene in these networks are shown in **Table 2**. Inter-relationships of genes in each of these pathway networks are shown in **Figure 2**. Network 1 functions in the cardiovascular system during development of function. Ubiquitin C plays a key role in network 1. Network 2 controls cellular growth and JNK is a central molecule of this network. Network 3 functions in cell morphology, in which P38 MARK and Rac are the central molecules. Network 4 controls gene expression and IL6

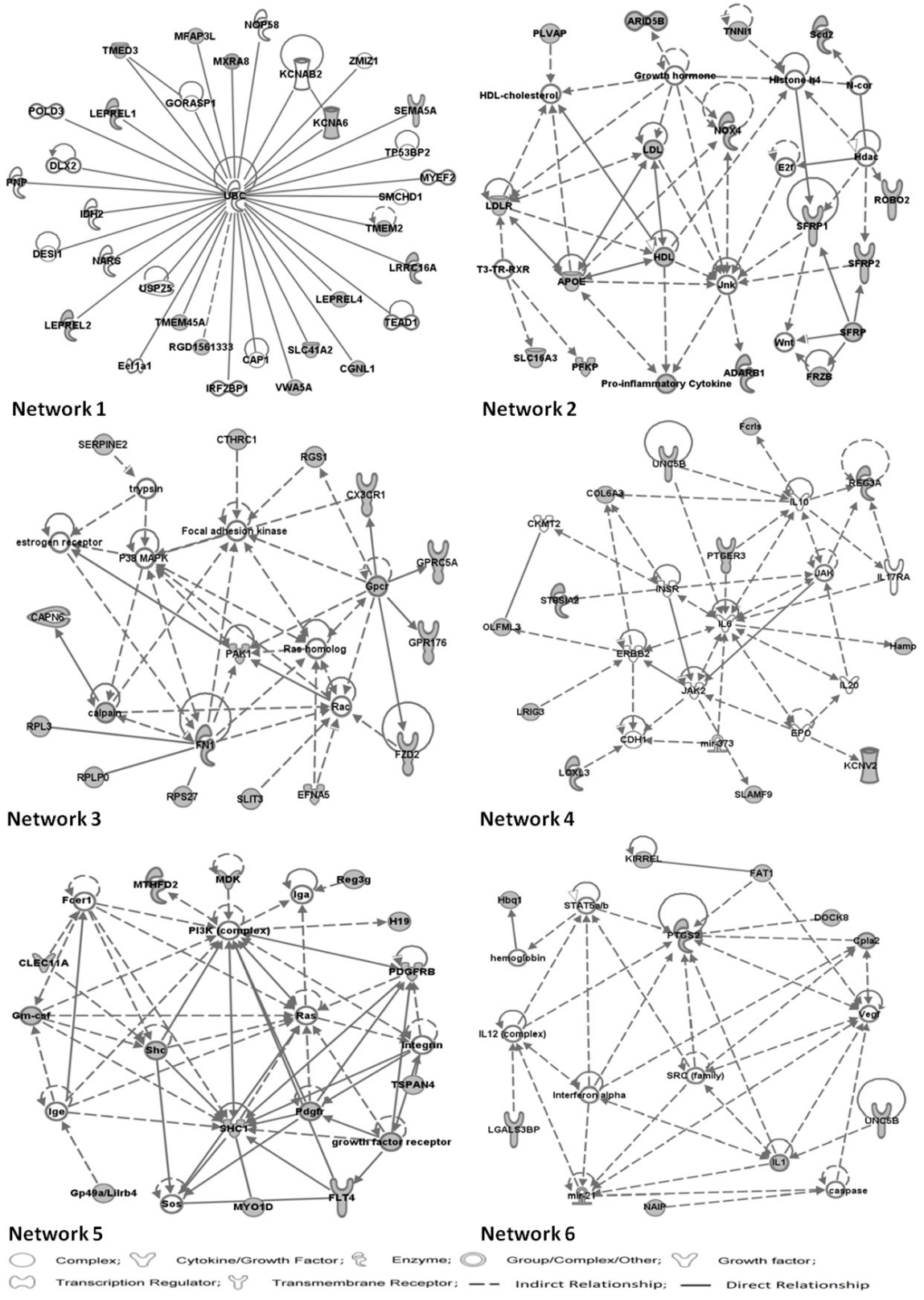


**Figure 2.** Pathway networks associated with the elevated genes in the surviving cardiomyocytes of the infarcted myocardium. Network 1 and 5 regulate cardiovascular system development and function. Network 2 controls cellular growth. Network 3 functions in cell morphology. Network 4 controls gene expression. Network 6 regulates cell death and survival.

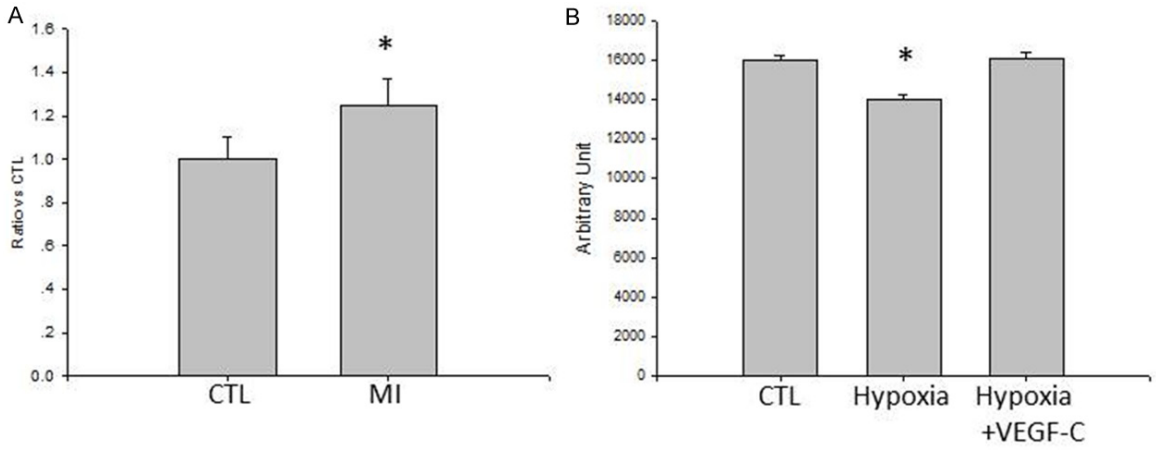


**Figure 3.** Regulation of VEGF-C on cardiomyocyte size. Compared to the normal myocardium, myocyte diameter is significantly increased in the infarcted myocardium at week 2 post-MI (panel A). In cultured cardiomyocytes, hypoxia significantly reduced cardiomyocyte size, which was prevented by VEGF-C treatment (panel B).

and JAK are the key molecules. The top function of network 5 is development and function of the cardiovascular system, in which the central molecules include the PI3K complex and Ras. The major function of network 6 is cell death and survival and VEGF is the key molecule of the network.

*Cardiomyocyte hypertrophy in the infarcted myocardium*

Compared to the normal myocardium, surviving cardiomyocyte diameter in the infarcted myocardium was significantly increased at week 2 post-MI (**Figure 3A**).

*Regulation of VEGF-C on cardiomyocyte size during hypoxia*

Potential regulation of VEGF-C on cardiomyocyte size was further determined in cultured neonatal cardiomyocytes. Under hypoxic conditions, neonatal cardiomyocyte size was significantly reduced compared to cells in normoxic conditions. VEGF-C treatment prevented cardiomyocyte atrophy during hypoxia (**Figure 3B**).

*Effect of VEGF-C on hypertrophic markers in neonatal cardiomyocytes*

ANP, BNP and β-MHC are markers of cardiomyocyte hypertrophy. Our qPCR data revealed that VEGF-C treatment significantly increased ANP and BNP mRNA levels compared to untreated cells (**Figure 4**). Western blot detection further showed that ANP and β-MHC levels in cardiomyocytes were also significantly elevated by VEGF-C treatment (**Figure 4**).

*Regulation of myocyte apoptosis by VEGF-C*

The potential regulation of VEGF-C on cardiomyocyte apoptosis was assessed in hypoxic conditions. Bax and caspases stimulate cell apoptosis. Compared to cardiomyocytes in normal conditions, hypoxia significantly increased Bax, cleaved caspase 3, 8 and 9, which were significantly suppressed by VEGF-C treatment (**Figure 5**).

## Discussion

Myocardial remodeling occurs in the infarcted myocardium following MI, primarily characterized by myocyte hypertrophy and fibrosis (scar formation). Myocyte hypertrophy occurring early following MI is an appropriate compensatory response to preserve ventricular function [21]. Many cardiomyocytes are able to survive in the infarcted myocardium. Our gene expression profiling data revealed numerous differentially expressed genes in the surviving cardiomyocytes of the infarcted myocardium during the early stages of MI, while most of them were up-regulated. IPA further identified that the altered genes were primarily related to p38 MAPK, PI3K, VEGF, and ubiquitin pathway networks. These observations indicated that multiple molecular and cellular actions are amenable in viable cardiomyocytes of the

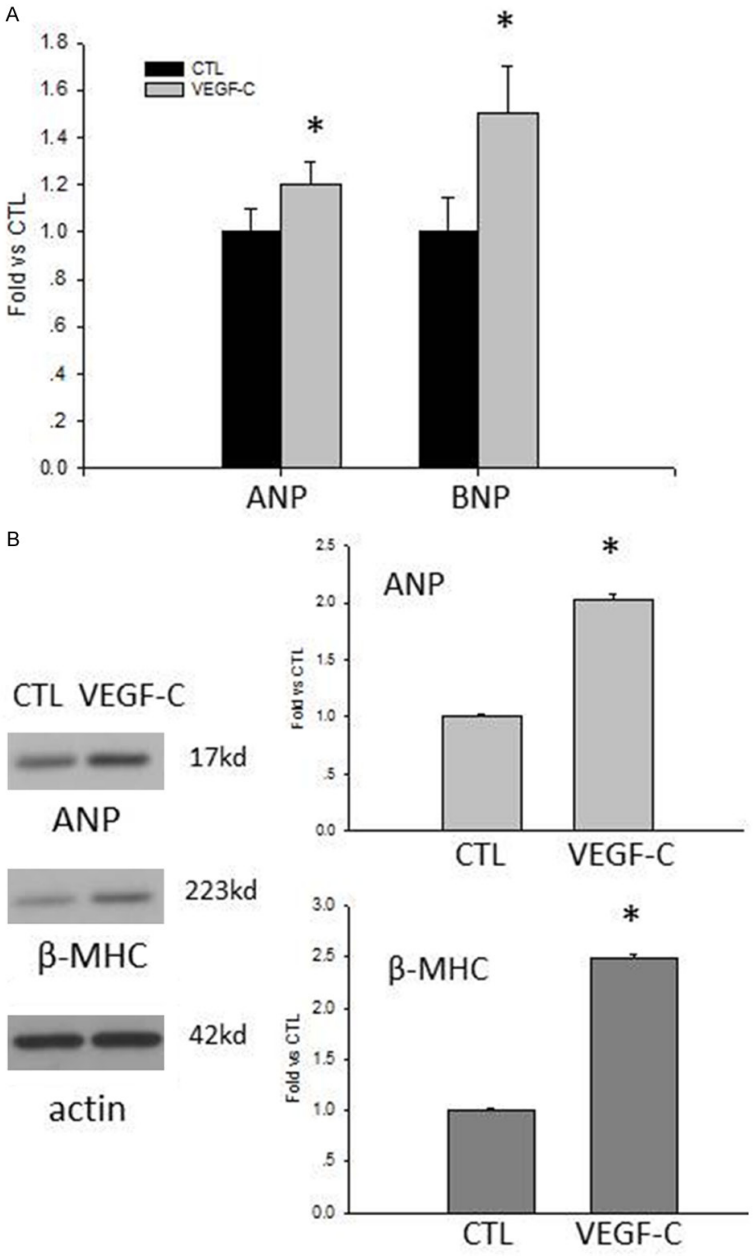


**Figure 4.** Effect of VEGF-C on hypertrophic markers in cardiomyocytes. VEGF-C treatment significantly increased ANP and BNP mRNAs (panel A), as well as ANP and β-MHC protein levels (panel B) compared to untreated cells.

infarcted myocardium, which are mediated by various pathways. Top functions of these networks are associated with cardiovascular development and function, cellular growth/survival and cell morphology. The current study further showed that ANP and BNP, markers of myocyte hypertrophy, are significantly elevated in surviving cardiomyocytes of the infarcted myocardium, which is accompanied with increased cardiomyocyte size (hypertrophy). Therefore, compensatory cardiomyocyte hypertrophy developed in the infarcted myocardium during the early stages of MI, which may be beneficial to ventricular function.

Mechanisms regulating cardiomyocyte hypertrophy are not fully understood and multiple factors/pathways have been recognized to participate. Our previous study revealed significantly elevated VEGF-C and VEGFR-3 levels in the infarcted myocardium, indicating that VEGF-C plays a role in cardiac repair/remodeling in autocrine and/or paracrine manners. We further showed that cells contributing to the increase in VEGFR-3 at the infarcted myocardium were primarily surviving cardiomyocytes. This finding suggests that VEGF-C/VEGFR-3 may regulate myocyte growth/function and/or survival in the repairing myocardium following MI.

Next, we explored the potential role of VEGF-C on cardiomyocyte hypertrophy using cultured neonatal rat cardiomyocytes. Under normoxic conditions, VEGF-C treatment significantly increased the expression of the hypertrophic markers ANP and β-MHC in cardiomyocytes. This finding suggests that VEGF-C promotes myocyte hypertrophy in normal oxygen states.

We further revealed that cultured neonatal cardiomyocytes undergo atrophy during hypoxia. VEGF-C treatment prevented hypoxia-induced myocyte atrophy. Thus, in addition to lymphangiogenesis, VEGF-C also plays a role in stimulating myocyte growth in both normoxic and hypoxic conditions.

The involvement of other VEGF isoforms in the development of myocyte hypertrophy has previously been reported. VEGF-B induces compen-

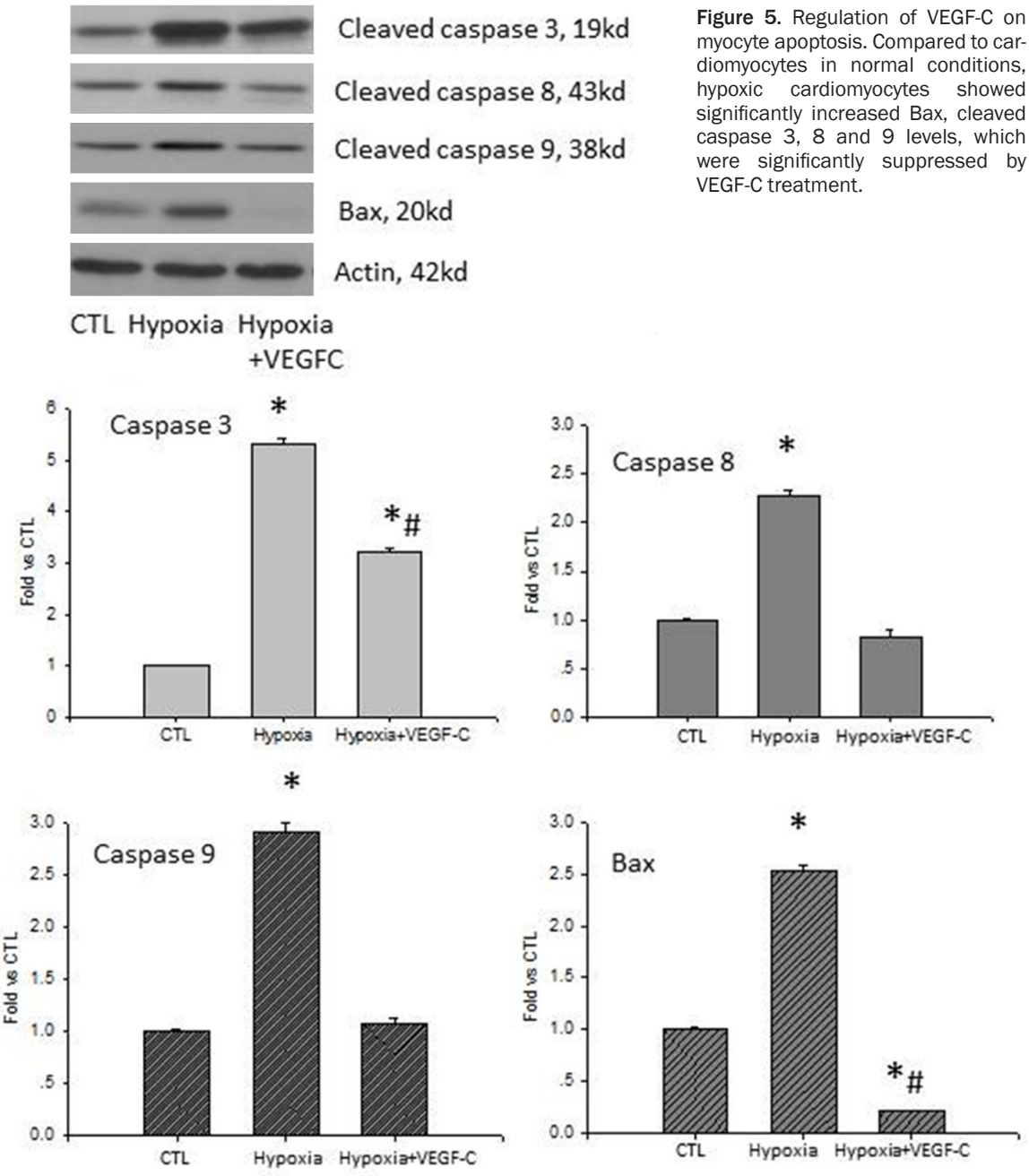


**Figure 5.** Regulation of VEGF-C on myocyte apoptosis. Compared to cardiomyocytes in normal conditions, hypoxic cardiomyocytes showed significantly increased Bax, cleaved caspase 3, 8 and 9 levels, which were significantly suppressed by VEGF-C treatment.

satory myocyte hypertrophy and preserves cardiac function following MI [22]. Moreover, prolonged overexpression of intramyocardial VEGF-A by gene transfection promotes cardiac contractility, preserves viable cardiac tissue, and prevents remodeling of the infarcted heart [23]. Therefore, multiple VEGF isoforms contribute to the development of myocyte hypertrophy in the infarcted heart.

Cardiomyocyte apoptosis plays a critical role in the pathogenesis of heart failure [24, 25]. Great attention has been focused on understanding the mechanisms of cardiomyocyte apoptosis with the ultimate goal of reducing the extent of injury and improving ventricular function. It has been hypothesized that apoptosis is responsible for a significant amount of cardiomyocyte death during the early stages of MI, as well as for a progressive loss of surviving cardiomyocytes during the subacute and chronic stages. Pharmacological and genetic inhibition of apoptosis has been shown to diminish infarct size and improve cardiac function [26, 27].

We then tested whether VEGF-C protects cardiomyocytes from apoptosis. Our results showed that under hypoxic conditions, the expression of the apoptosis markers Bax, caspase-3 and caspase-8 were significantly increased in cultured cardiomyocytes. Our data further revealed that VEGF-C treatment of hypoxic cardiomyocytes significantly suppressed caspases and Bax levels. These observations suggested that VEGF-C protects ischemic cardiomyocytes from apoptosis. Other members of the VEGF family have antiapoptotic effects in various tissues. VEGF-B mediated by VEGFR-1 has been reported to exert powerful antiapoptotic effects in both cultured cardiomyocytes and the infarcted myocardium [22]. $VEGF\text{-}B_{167}$ in nonischemic dilated cardiomyopathy limits apoptotic cell loss and delays the progression toward failure [28]. Inhibition of VEGFR-2 causes lung cell apoptosis [29]. Moreover, VEGF-B treatment can rescue neurons from apoptosis in the retina and brain in mouse models of ocular neurodegenerative disorders and stroke [30], respectively. Taken together, VEGF isoforms play an antiapoptotic role in various pathological conditions.

In summary, surviving cardiomyocytes within the infarcted heart expressed high levels of VEGFR-3 and developed compensatory hypertrophy during the early stages of MI. Our *in vitro* study further demonstrated that VEGF-C promotes cardiomyocyte hypertrophy and survival during hypoxia. Thus, VEGF-C is involved in other cellular mechanisms besides lymphangiogenesis. These findings indicated that VEGF-C may potentially offer a new therapeutic option for the treatment of ischemic cardiac disease. Further study is required to investigate the protective role of VEGF-C on the infarcted heart using VEGF-C treatment or VEGFR blockade.

## Acknowledgements

This work was supported by NIH Heart, Blood, and Lung Institute (1RO1-HL096503, Y. S.).

**Address correspondence to:** Dr. Yao Sun, Division of Cardiovascular Diseases, Department of Medicine, University of Tennessee Health Science Center, 956 Court Ave, Room B324, Memphis, TN 38163, USA. Tel: 901-448-4921; Fax: 901-448-4921; E-mail: yasun@uthsc.edu

## References

[1] Minicucci MF, Azevedo PS, Polegato BF, Paiva SA, Zornoff LA. Heart failure after myocardial infarction: clinical implications and treatment. Clin Cardiol 2011; 34: 410-414.

[2] Sun Y. Myocardial repair/remodelling following infarction: roles of local factors. Cardiovasc Res 2009; 81: 482-490.

[3] Hori M, Nishida K. Oxidative stress and left ventricular remodelling after myocardial infarction. Cardiovasc Res 2009; 81: 457-464.

[4] Jeremy JY, Shukla N, Muzaffar S, Handley A, Angelini GD. Reactive oxygen species, vascular disease and cardiovascular surgery. Curr Vasc Pharmacol 2004; 2: 229-236.

[5] Coso S, Bovay E, Petrova TV. Pressing the right buttons: signaling in lymphangiogenesis. Blood 2014; 123: 2614-2624.

[6] Shibuya M. Vascular endothelial growth factor and its receptor system: physiological functions in angiogenesis and pathological roles in various diseases. J Bio chem 2013; 153: 13-19.

[7] Dias S, Choy M, Alitalo K, Rafii S. Vascular endothelial growth factor (VEGF)-C signaling through FLT-4 (VEGFR-3) mediates leukemic cell proliferation, survival, and resistance to chemotherapy. Blood 2002; 99: 2179-2184.

[8] Takenouchi K, Shrestha B, Yamakuchi M, Yoshinaga N, Arimura N, Kawaguchi H, Nagasato T, Feil R, Kawahara K, Sakamoto T,Maruyama I, Hashiguchi T. Upregulation of non-beta Cell-derived Vascular Endothelial Growth Factor A Increases Small Clusters of Insulin-producing Cells in the Pancreas. Exp Clin Endocrinol Diabetes 2014; 122: 308-315.

[9] Zhao T, Zhao W, Meng W, Liu C, Chen Y, Sun Y. Vascular endothelial growth factor-C: its unrevealed role in fibrogenesis. Am J Physiol Heart Circ Physiol 2014; 306: H789-796.

[10] Zhao T, Zhao W, Chen Y, Liu L, Ahokas RA, Sun Y. Differential expression of vascular endothelial growth factor isoforms and receptor subtypes in the infarcted heart. Int J Cardiol 2013; 167: 2638-2645.

[11] Zhao T, Zhao W, Chen Y, Ahokas RA, Sun Y. Vascular endothelial growth factor (VEGF)-A: role on cardiac angiogenesis following myocardial infarction. Microvasc Res 2010; 80: 188-194.

[12] Moey M, Gan XT, Huang CX, Rajapurohitam V, Martinez-Abundis E, Lui EM, Karmazyn M. Ginseng reverses established cardiomyocyte hypertrophy and postmyocardial infarction-induced hypertrophy and heart failure. Circ Heart Fail 2012; 5: 504-514.

[13] Chen H, Liu Z, Gong S, Wu X, Taylor WL, Williams RW, Matta SG, Sharp BM. Genome-Wide Gene Expression Profiling of Nucleus Accumbens Neurons Projecting to Ventral Pallidum Using both Microarray and Transcriptome Sequencing. Front Neurosci 2011; 5: 98.

[14] Zhao W, Zhao T, Chen Y, Qu Y, Gerling IC, Sun Y. Modification of oxidative stress on gene ex-

pression profiling in the rat infarcted heart. Mol Cell Biochem 2013; 379: 243-253.
[15] Wu J, Kakoola DN, Lenchik NI, Desiderio DM, Marshall DR, Gerling IC. Molecular phenotyping of immune cells from young NOD mice reveals abnormal metabolic pathways in the early induction phase of autoimmune diabetes. PLoS One 2012; 7: e46941.
[16] Zhao T, Zhao W, Chen Y, Ahokas RA, Sun Y. Acidic and basic fibroblast growth factors involved in cardiac angiogenesis following infarction. Int J Cardiol 2011; 152: 307-313.
[17] Sun M, Ouzounian M, de Couto G, Chen M, Yan R, Fukuoka M, Li G, Moon M, Liu Y, Gramolini A, Wells GJ, Liu PP. Cathepsin-L ameliorates cardiac hypertrophy through activation of the autophagy-lysosomal dependent protein processing pathways. J Am Heart Assoc 2013; 2: e000191.
[18] Luo D, Yang D, Lan X, Li K, Li X, Chen J, Zhang Y, Xiao RP, Han Q, Cheng H. Nuclear Ca2+ sparks and waves mediated by inositol 1,4,5-trisphosphate receptors in neonatal rat cardiomyocytes. Cell Calcium 2008; 43: 165-174.
[19] Kang PM, Haunstetter A, Aoki H, Usheva A, Izumo S. Morphological and molecular characterization of adult cardiomyocyte apoptosis during hypoxia and reoxygenation. Circ Res 2000; 87: 118-25.
[20] Braz JC, Bueno OF, De Windt LJ, Molkentin JD. PKC alpha regulates the hypertrophic growth of cardiomyocytes through extracellular signal-regulated kinase1/2 (ERK1/2). J Cell Biol 2002; 156: 905-919.
[21] Sutton MG, Sharpe N. Left ventricular remodeling after myocardial infarction: pathophysiology and therapy. Circulation 2000; 101: 2981-2988.
[22] Zentilin L, Puligadda U, Lionetti V, Zacchigna S, Collesi C, Pattarini L, Ruozi G, Camporesi S, Sinagra G, Pepe M, Recchia FA, Giacca M. Cardiomyocyte VEGFR-1 activation by VEGF-B induces compensatory hypertrophy and preserves cardiac function after myocardial infarction. FASEB J 2010; 24: 1467-1478.
[23] Madonna R, De Caterina R. VEGF receptor switching in heart development and disease. Cardiovasc Res 2009; 84: 4-6.
[24] van Empel VP, Bertrand AT, Hofstra L, Crijns HJ, Doevendans PA, De Windt LJ. Myocyte apoptosis in heart failure. Cardiovasc Res 2005; 67: 21-29.
[25] Chiong M, Wang ZV, Pedrozo Z, Cao DJ, Troncoso R, Ibacache M, Criollo A, Nemchenko A, Hill JA, Lavandero S. Cardiomyocyte death: mechanisms and translational implications. Cell Death Dis 2011; 2: e244.
[26] Perrin C, Ecarnot-Laubriet A, Vergely C, Rochette L. Calpain and caspase-3 inhibitors reduce infarct size and post-ischemic apoptosis in rat heart without modifying contractile recovery. Cell Mol Biol (Noisy-le-grand) 2003; 49 Online Pub: OL497-505.
[27] Zhao ZQ, Morris CD, Budde JM, Wang NP, Muraki S, Sun HY, Guyton RA. Inhibition of myocardial apoptosis reduces infarct size and improves regional contractile dysfunction during reperfusion. Cardiovasc Res 2003; 59: 132-142.
[28] Pepe M, Mamdani M, Zentilin L, Csiszar A, Qanud K, Zacchigna S, Ungvari Z, Puligadda U, Moimas S, Xu X, Edwards JG, Hintze TH, Giacca M,Recchia FA. Intramyocardial VEGF-B167 gene delivery delays the progression towards congestive failure in dogs with pacing-induced dilated cardiomyopathy. Circ Res 2010; 106: 1893-1903.
[29] Kasahara Y, Tuder RM, Taraseviciene-Stewart L, Le Cras TD, Abman S, Hirth PK, Waltenberger J, Voelkel NF. Inhibition of VEGF receptors causes lung cell apoptosis and emphysema. J Clin Invest 2000; 106: 1311-1319.
[30] Li Y, Zhang F, Nagai N, Tang Z, Zhang S, Scotney P, Lennartsson J, Zhu C, Qu Y, Fang C, Hua J, Matsuo O, Fong GH, Ding H, Cao Y, Becker KG, Nash A, Heldin CH, Li X. VEGF-B inhibits apoptosis via VEGFR-1-mediated suppression of the expression of BH3-only protein genes in mice and rats. J Clin Invest 2008; 118: 913-923.